

## Mid-Infrared Sky Brightness Site Testing at the South Pole

CRAIG H. SMITH

School of Physics, University College, UNSW, Australian Defence Force Academy, Canberra, ACT, 2600, Australia; c-smith@adfa.oz.au

AND

DOYAL A. HARPER

University of Chicago, Yerkes Observatory, Williams Bay, WI 53191; al@hale.yerkes.uchicago.edu

*Received 1996 December 15; accepted 1997 May 2*

**ABSTRACT.** During the austral summer of 1996, the mid-infrared imaging polarimeter NIMPOL was operated at the Amundsen-Scott South Pole Station, to obtain quantitative measurements of the 10 and 20  $\mu\text{m}$  sky brightness and stability. These observations were conducted as part of the Joint Australian Centre for Astrophysical Research in Antarctica (JACARA) site testing program on the Antarctic Plateau. The results of this site testing program are presented. The observations show that the mid-infrared sky brightness at the South Pole Station is much less than comparison sky brightness observations made at the Canberra base of the instrument. This reduction in sky brightness is attributed largely to the low emissivity of the atmosphere (because of its dryness and lack of aerosols), and the effect of the reduced atmospheric temperature (there is an expected decrease by a factor of 2.5 from the temperature difference between the two sites alone). The measured 11  $\mu\text{m}$  sky emissivity at the South Pole is also lower than previous measurements of the sky emissivity at Mauna Kea Observatory in Hawaii. The sky brightness was also found to be more stable than at the warmer, mid-latitude site (Canberra), and it is expected that “stare” mode operation of the instrument for astronomical observations would be quite feasible under these conditions. Measurements were also made during a period of “ice haze,” and the suspended ice crystals were observed to increase the sky background by 16% compared with clear weather and to add low-frequency brightness variations. However, this variability could be removed by slow (2 Hz) chopping, allowing high-sensitivity observing to continue through the “ice haze.”

### 1. INTRODUCTION

Mid-infrared astronomical observations from the ground are almost always background-limited by the strong thermal emission from the sky itself. That is, the photon shot noise from the warm background sky (and telescope structure) is usually many times larger than the astronomical signal of interest, and this background sets a fundamental sensitivity limit. Significantly higher sensitivities can be obtained by space-based instruments, where there is no thermal emission from the Earth’s atmosphere, although cryogenic telescopes are then required to keep the telescope emission down. However, the cost of these spaceborne missions is prohibitive to all but multinational consortiums. Furthermore, space-based missions are limited to fairly short lifetimes by the need to carry liquid cryogenics (e.g., the *Infrared Space Observatory* [ISO] had an expected lifetime of 18 months). Finally, such telescopes are also severely limited in spatial resolution by the size of the cooled telescope mirror (e.g., the diffraction limit at 10  $\mu\text{m}$  for a 4 m class telescope is about  $0''.54$ , whereas for ISO, with a 0.6 m mirror, it is 6.5 times larger at  $3''.5$ ). So ground-based mid-infrared astronomy has a long future before the spatial resolution obtainable on the ground is overhauled by a space-based system, if ever.

To maximize the sensitivity of ground-based mid-infrared observations we look to site telescopes at observatories with the darkest infrared skies. The major contribution to the large background for ground-based systems is the thermal emission from the warm atmosphere, and in particular the water vapor content, since water vapor has many strong absorption/emission bands in this region of the spectrum. To minimize the effects of water vapor, we use telescopes at high cold and dry sites. Recently, Ashley et al. (1996) and Nguyen et al. (1996) have shown that there are spectacular gains in sensitivity to be made in the near-infrared region of the spectrum (1–5  $\mu\text{m}$ ) by observing from the extremely cold and dry Antarctic Plateau, and they find order-of-magnitude sensitivity improvements in the *K* band at the South Pole. The South Pole is located at an altitude of 2800 m on the Antarctic Plateau, which is one of the driest deserts in the world, with an annual snow precipitation of less than 5  $\text{cm yr}^{-1}$ . The surface temperatures range from summertime temperatures of around  $-30^\circ\text{C}$  to below  $-70^\circ\text{C}$  in the winter, and the precipitable water vapor (PWV) content averages around 300  $\mu\text{m}$ . Being situated near Dome Argus, the highest point and source of the katabatic winds on the plateau, the wind velocities are generally low, and average

around 5 knots. These characteristics combine to make the Antarctic Plateau a potentially superb site for infrared astronomy.

The gains in sensitivity in the near-IR are impressive, but it is expected that such large gains may not be obtainable at mid-infrared wavelengths. This is because the near-infrared wavelengths lie on the steeply rising Wien side of the blackbody curve for atmospheric temperatures, so relatively modest reductions in temperature (i.e., from around 273 to 210 K) produce huge drops in the emission from the atmosphere, providing the order-of-magnitude sensitivity improvements quoted. The thermal wavelengths (5–20  $\mu\text{m}$ ) sit at the crest of the blackbody curves for these temperatures, so the same temperature drop produces a more modest background reduction, a factor of between 2 and 6, comparing the temperatures at a good, mid-latitude site such as Mauna Kea, Hawaii (0°C to +5°C), with that at the South Pole (–30°C to –70°C). However, one of the major problems for mid-infrared, mid-latitude astronomy is the inherently unstable nature of the sky background caused by microthermal turbulence and changes in temperature and in water vapor and aerosol content. At the South Pole this variability is expected to be a minimum due to the lack of diurnal temperature variations, light winds, and complete snow cover. Finally, the water vapor content, even at 4200 m altitude at Mauna Kea Observatory, cuts deeply into the atmospheric windows; this means the 20  $\mu\text{m}$  window, which contains some important astrophysical emission lines (e.g., molecular hydrogen), is only occasionally usable and relies on the serendipitous scheduling of a mid-infrared instrument when the usable conditions are present. On the Antarctic Plateau it is expected that the lower water vapor content would make 20  $\mu\text{m}$  observations routinely feasible and perhaps reduce the sky emission in the 10  $\mu\text{m}$  region by more than the simple ratio of blackbody temperatures by lowering the effective emissivity of the sky.

However, these benefits need to be quantified, and particularly the effect of blowing snow or “ice haze” needs to be determined. It is possible that the presence of this “ice haze” (which is variable and emitting strongly at mid-infrared wavelengths), could completely negate any benefits from going to the Antarctic Plateau. No quantitative data exists prior to this paper to confirm or refute this possibility.

To provide quantitative data about the Antarctic mid-infrared sky brightness and stability, the Imaging Polarimeter, NIMPOL, (developed at the University College of UNSW) was deployed to the South Pole for three weeks in 1996 January. At these wavelengths the effect of sunlight is negligible so it was possible to take advantage of the excellent logistic support of the US Amundsen-Scott South Pole Station over the summer. This experiment was conducted as part of the Joint Australian Centre for Astrophysical Research in Antarctica (JACARA) site testing program on the Antarctic Plateau and complements the near-infrared sky brightness measurements of Ashley et al. (1996). This experiment enjoyed the considerable support of the US

Center for Astrophysical Research in Antarctica (CARA), which supplied all of the logistical support for this site testing campaign.

## 2. INSTRUMENT SETUP

The NIMPOL Imaging Polarimeter is a mid-infrared imaging system designed primarily for astronomical polarimetric imaging, but also for plain imaging as required. The instrument has been operated at a number of major astronomical observatories since 1993. See Smith, Aitken, & Moore (1994) or Smith et al. (1996) for detailed descriptions of the instrument and examples of observational results to date.

The instrument is based on an Amber Engineering, USA 128 × 128 Si:Ga FPA. The detector is cooled to 18 K in a helium-cooled cryostat, as are all associated optics. The optics are transmissive, and normally provide diffraction-limited imaging performance on a 4 m telescope. At the South Pole the instrument was set up without a telescope, and the normal input optics of the instrument provided a beam size of 1% on the sky. An external 45° rotatable mirror was used to direct the beam to various elevations on the sky. Wavelength selection was made by a selection of narrowband and broadband filters and an 8–14  $\mu\text{m}$  circular variable filter (CVF). The instrument was run by a PC for general instrument control and data display, and TMS320C25/50 digital signal processors for generating clock signals for the detector and the fast data acquisition.

The ambient temperature at the South Pole during January was about –35°C, which is enough to freeze normal “viton” O-rings, causing failure of the vacuum, and well below the –7°C specification for the Ferrofluidic seals used for the filter and CVF drive shafts. To avoid replacing all of the Dewar O-rings with fluorosilicone O-rings and reengineering the drive shaft seals, it was considered expedient to keep the cryostat “warm.” This was achieved by mounting the instrument in a well-insulated and heated box, with a snout through which the instrument “looked” out to the sky (see Fig. 1). The temperature inside the box was maintained at –5°C, with a temperature controller and heating tape. The computer and DSPs that run the instrument normally hang beside the cryostat on a telescope, but in this case the electronics and computers were housed inside the warm Martin A. Pomerantz Observatory (MAPO) building. All cabling was replaced with Teflon plenum, which remains flexible at the low polar temperatures. This instrument configuration worked extremely well, and there were no instrument problems throughout the site testing period. However, the rigors of regular helium transfers into the Dewar under the prevailing weather conditions (especially in the winter) should not be underestimated, and future instruments to be deployed at the South Pole might well consider the benefits of using closed-cycle cooler systems, which also provide the logistical benefits of not requiring air transportation and storage of large quantities of liquid cryogenics.



FIG. 1.—NIMPOL, in its insulated and heated box, on the top of the MAPO building, at the US Amundsen-Scott base at the South Pole.

### 3. OBSERVATIONAL RESULTS

The objectives of the mid-infrared site testing program were to obtain quantitative measurements of the sky brightness in the  $N$  8–13  $\mu\text{m}$  and  $Q$  16–22  $\mu\text{m}$  windows, to determine the stability of the mid-infrared sky, and to determine the effects of “ice haze” on the sky brightness and stability. Throughout the observing period 1996 January 15–28 the ambient temperature was between  $-30^\circ\text{C}$  and  $-35^\circ\text{C}$  and only varied slowly from day to day, and of course there were no diurnal heating effects.

#### 3.1. Sky Brightness

The sky brightness was measured continuously on each day that was clear of cloud and was found to vary little from day to day. Measurements of the sky brightness in each of the filters are presented in Table 1. The 8.5 and 12.5  $\mu\text{m}$  filters represent the edges of the 8–13  $\mu\text{m}$  window, and the 11.5  $\mu\text{m}$  filter is placed in the “best” part of this window. Both the actual sky brightness, and the effective sky emissivity with respect to a  $-30^\circ\text{C}$  blackbody are shown. The 17  $\mu\text{m}$  filter provides an

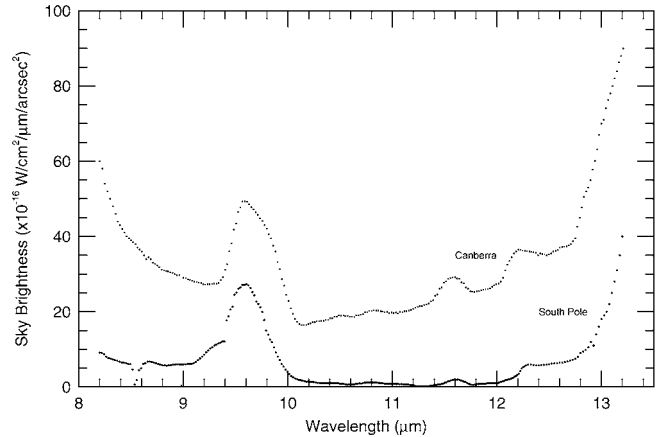


FIG. 2.—CVF spectrum from 8 to 13  $\mu\text{m}$  of the sky brightness at the South Pole and Canberra. In the “cleanest” part of the window (between 10.5 and 12  $\mu\text{m}$  the South Pole sky brightness is a factor of 20–40 less than that observed on a clear night in Canberra.

indication of how clean the 20  $\mu\text{m}$  window is, and at mid-latitude sites this filter generally shows the sky to be at least 50% emissive. For comparison, Table 1 also shows the sky brightness and emissivity obtained with the same experimental setup on a perfectly clear night at the Canberra base of the instrument. These results represent a sky temperature of  $10^\circ\text{C}$ , relative humidity 35%, and altitude 600 m. Figure 2 shows the sky emissivity from 8 to 13  $\mu\text{m}$ , obtained through the CVF. The large bump at 9.7  $\mu\text{m}$  is caused by emission from atmospheric ozone.

Because the sky background is so low at the South Pole, particularly in the 11.5  $\mu\text{m}$  filter, the greatest challenge in making these measurements was to determine the contributions of the “warm” Dewar window (at  $T \approx -5^\circ$ ) and  $45^\circ$  angle mirror (at  $T \approx -30^\circ$ ). The emissivity of these components was measured by making the Dewar “look” through the same optical path, into a liquid nitrogen reservoir, which effectively provides no thermal signal. The measured signal, compared with a true null signal (determined from a cold blank at 4 K inside the Dewar) then represents the contributions of the Dewar lens and  $45^\circ$  mirror. The effective instrumental emissivity measured in

TABLE 1  
SKY BRIGHTNESS MEASUREMENTS

FILTER NAME	$\lambda_0$ ( $\mu\text{m}$ )	$\Delta\lambda$ ( $\mu\text{m}$ )	SOUTH POLE		CANBERRA		SYSTEM EMISSIVITY (%)
			Sky Flux ( $\text{Jy arcsec}^{-2}$ )	Emissivity <sup>a</sup> (%)	Sky Flux ( $\text{Jy arcsec}^{-2}$ )	Emissivity <sup>b</sup> (%)	
$N$ band	10.6	5.8	494	19.7	1369	23.5	11.1
17 $\mu\text{m}$ BB	17.0	2.0	1227	20.4	5093	50.7	34.3
8.5 $\mu\text{m}$ NB	8.5	1.0	122	8.5	596	15.5	9.6
11.5 $\mu\text{m}$ NB	11.5	1.0	25	0.7	468	6.3	8.9
12.5 $\mu\text{m}$ NB	12.5	1.0	815	19.3	2792	33.5	11.4

<sup>a</sup> Referenced to an ambient temperature  $-30^\circ\text{C}$  blackbody.

<sup>b</sup> Referenced to an ambient temperature  $10^\circ\text{C}$  blackbody.

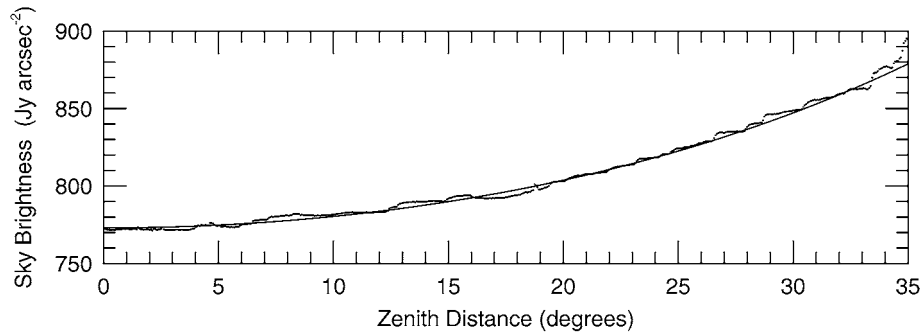


FIG. 3.—Skydip measurements at the  $N$  band ( $8\text{--}13\ \mu\text{m}$ ) show the sky brightness vs. zenith distance. The dots show the observed data, and the solid curve shows a  $\sec z$  curve normalized to the  $0^\circ$  zenith distance observation. An excellent correlation between the sky brightness and air mass is observed.

this way is referenced to a blackbody at the ambient temperature. The main uncertainty or difficulty in this experimental setup is ensuring that stray light does not enter the system and thereby raise the calculated emissivity of the mirror/lens system, but with some care this can be determined to better than 1%. The combined mirror and lens emissivity of the system at each filter wavelength is included in Table 1, but the sky brightness and emissivities presented have had the instrumental component removed.

The  $11.5\ \mu\text{m}$  data (Table 1) and CVF spectra (Fig. 2) show dramatic decreases in the sky brightness at the South Pole compared with the mid-latitude Canberra observations. The sky brightness is 10–20 times less, and much less than the value predicted (about a factor of 2.5) from the temperature difference alone between the two sites. This significant decrease in the sky emissivity at the South Pole can be attributed to the lower water vapor and aerosol content. The smaller changes in emissivity in the  $8.5$ ,  $12.5$ ,  $17\ \mu\text{m}$ , and  $N$ -band filters is expected because these filters cover wavelength regions that still contain saturated water vapor bands, so here the background changes derive largely from the temperature decrease, without as much of the corresponding emissivity decrease.

Comparing the South Pole with infrared observations taken at Canberra is perhaps a little unfair, since Canberra (though perhaps under-rated) is not a renowned infrared site, and the sky brightness observations need to be repeated at an existing “good” observing site. To date, though, we do not have equivalent data taken from a good site like Mauna Kea, although it is planned to obtain such data in the next 12 months. The only comparison we have with Mauna Kea data is unpublished emissivity measurements (by Roche, Smith, and Aitken) made from the United Kingdom Infrared Telescope (UKIRT) in 1991 November with the UCL spectrometer (see Aitken & Roche 1982 for details of this instrument). These measurements were made through the telescope with a different instrument and so are not exactly comparable, but they do provide a rough comparison. After subtracting the instrument and telescope emissivities, we obtained a sky emissivity between  $11$  and  $12\ \mu\text{m}$  (cf.  $11.5\ \mu\text{m}$  narrowband filter) of 6.3% for  $T = 3.5^\circ\text{C}$  and

PWV = 5 mm on 1992 November 15 and 2.5% for  $T = 5^\circ\text{C}$  and PWV = 2 mm on 1991 November 18. The conditions for November 15 would have been considered “average,” and for November 18 conditions were “very good, and dry.” From these results, the Canberra sky emissivity in the  $11\text{--}12\ \mu\text{m}$  region (taken on a clear dry night) is similar to an average Mauna Kea night. As yet we do not have sky brightness stability data for Mauna Kea.

### 3.2. Sky Brightness from Skydips

Another way to account for the constant contribution of the instrumental emissivity is to use what is generally called the technique of “skydips.” Here the  $45^\circ$  mirror is rotated so that the beam from the instrument scans in elevation, presenting a changing air mass to the instrument field of view. A time sequence shows a constant component because of the instrumental emissivity, and a component due to the sky emission that varies as the air mass, or  $\sec z$ , where  $z$  is the zenith distance in degrees.

Skydip measurements were obtained, although the elevation scans were limited to about  $\pm 35^\circ$  from the zenith by the handrails around the top of the MAPO building, which obstructed the clear field of view. Figure 3 shows the skydip observations as a function of zenith distance, and the solid curve shows the  $\sec z$  dependence normalized to the  $z = 0^\circ$  measurement. Excellent agreement with the  $\sec z$  curve was evidenced by the skydip data. These observations were made with the  $N$ -band ( $\Delta\lambda = 5.8\ \mu\text{m}$ ) filter, and the sky and instrumental emissions determined in this way (20.4% and 10.4%, respectively, of a  $-30^\circ$  blackbody) match those found in Table 1 very well (to within 0.5%).

### 3.3. Sky Stability

The other main experiment, besides determining the absolute sky brightness at the South Pole, was to determine the stability of the mid-infrared sky. To achieve this, time sequences with 50 ms integration times were obtained over many hours. Figure 4a shows a representative plot of the sky stability during pe-

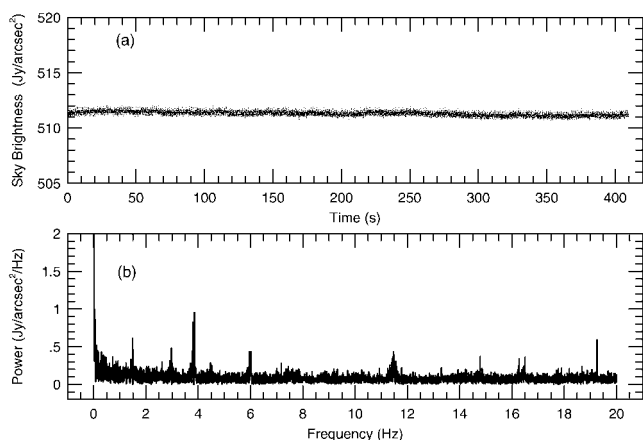


FIG. 4.—(a) Sky stability in the  $N$ -band at the South Pole with 50 ms integrations, at  $0^\circ$  zenith distance. The  $N$ -band sky is very flat and stable with time. The noise on the otherwise flat distribution is photon shot noise from the sky emission, though this noise is hard to see in the Canberra data, owing to the large-scale variations in brightness. (b) Power spectrum vs. frequency from (a). The DC component has been removed from the power spectrum.

riods of very clear weather in the  $N$  band, and Figure 5a shows a similar plot for a clear Canberra night. Figures 4b and 5b show the power spectrum versus frequency for the sky brightness data, after the DC term has been removed.

Clearly, the South Pole sky even in summer was very much more stable than the mid-latitude site. The noise superimposed on the basically flat curve in Figure 4a is photon shot noise from the sky emission, though this noise is hard to see in the Canberra data, owing to the large-scale variations in brightness. Features near 4 and 12 Hz in the power spectra undoubtedly refer to some sort of electronic noise, though the power in these features is inconsequential compared with the total power in the spectrum. Perhaps a little surprisingly, most of the variations (even in the Canberra data) are at quite low frequencies (2 Hz or less). Traditionally, sky chopping at mid-infrared wavelengths has been at rates of 10 Hz or more, but from these data, chopping rates of as low as 2 Hz would be quite adequate to remove most of the unwanted sky variability. Käufel et al. (1991) found similar slow sky variations from observations at the ESO observatory in Chile, although they estimated a minimum chopping frequency of 8 Hz was required. At the South Pole, we see that the power spectrum does not rise until less than 0.5 Hz, and under these conditions chopping would probably not be necessary, since all sky variability corrections could be made quite slowly in a stare observing mode. Removing the need for chopping would be a major simplification in telescope design and construction and improves observing efficiency from 50% to 100%.

It should be noted that these observations were made in a  $1.8''$  beam, so some smoothing of the temporal variations may be anticipated compared with the arcsecond-sized beam that one would actually use for astronomical observations. However, until we have a telescope large enough (2–4 m) to produce

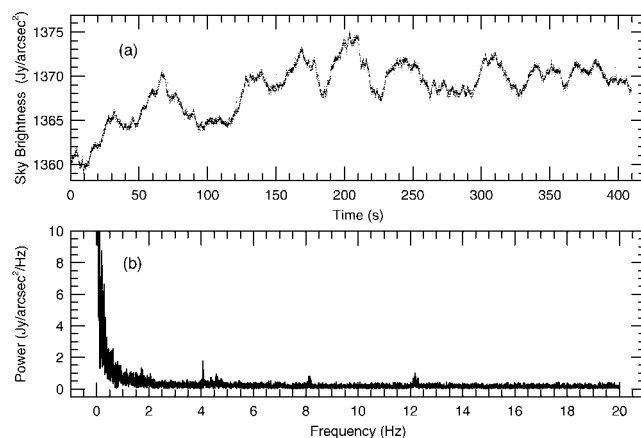


FIG. 5.—(a) Sky stability in the  $N$ -band on a “perfect,” clear night in Canberra, with 50 ms integrations, at  $0^\circ$  zenith distance. (b) Power spectrum vs. frequency from (a). The DC component has been removed from the power spectrum.

arcsecond-sized beams at these wavelengths, these observations must suffice.

Figures 6a and 6b show the sky brightness versus time and power versus frequency at  $17 \mu\text{m}$  at the South Pole. At these wavelengths the Si:Ga detector’s quantum efficiency is significantly less than in the 8–13  $\mu\text{m}$  region, so longer integrations were required to remain background limited, even though the sky is actually brighter at these wavelengths. Integration times of 250 ms were used, and the total scan was some 2000 s long. There is clearly much more noise at all the measured frequencies than at 10  $\mu\text{m}$ , but certainly not impossible amounts. One curious feature, not seen in the scans at shorter wavelengths, is a quite strong 0.1/0.2 Hz feature. The origin of this feature

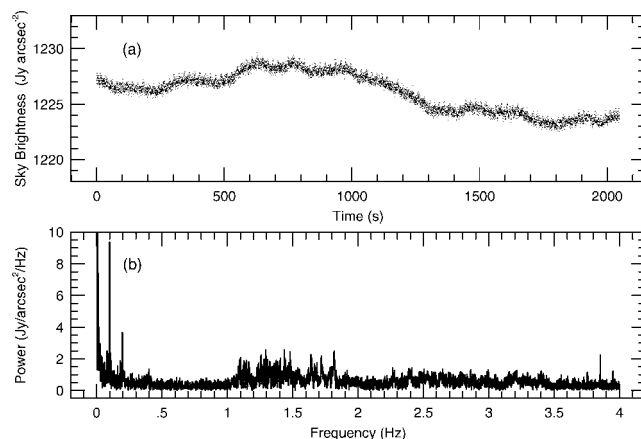


FIG. 6.—(a) Sky stability at  $17 \mu\text{m}$  at the South Pole with 250 ms integrations, at  $0^\circ$  zenith distance. (b) Power spectrum vs. frequency from (a). The DC component has been removed from the power spectrum. The origin of the strong periodic feature at 0.1/0.2 Hz (10/5 s intervals in [a]) is unclear but is presumably man-made, perhaps building shake.

is not clear, though it is presumably a man-made signal, perhaps building shake. It should also be noted that the filter used here also cuts into the deep atmospheric water vapor absorption/emission at  $16\ \mu\text{m}$ , so these results are most encouraging, and a custom filter that avoided all of the main absorption bands would undoubtedly provide even more stable  $20\ \mu\text{m}$  conditions.

Similar observations obtained from a good infrared observatory site would be a valuable comparison, and such observations will be made from Mauna Kea, Hawaii, if funds to support such measurements can be obtained.

### 3.4. Ice Haze

On 1996 January 21 ice crystals were clearly, visually observed in an otherwise clear sky. A number of  $N$ -band time series scans were obtained during this period, and one such scan is presented in Figure 7a. The sky brightness is increased by a factor of about 16% compared with Figure 4 taken in clear weather, and low-frequency brightness variations are evident. It should be noted that although the total increase in  $N$ -band brightness caused by the ice haze is quite modest, it is probable that a much larger proportional increase would be expected in the best part of the window ( $10.5\text{--}12\ \mu\text{m}$ ). The power spectrum in Figure 7b shows quite strong features at 6 and 16 Hz, and a large increase in power at frequencies less than 2 Hz. The “turn-up” at 2 Hz is clearly a result of the variations in sky background caused by the “ice haze,” but the identity of the narrow features at 6 and 16 Hz is unclear, though it is possible that these features are associated with the “ice haze.” As might be expected, these observing conditions are significantly worse than those during “clear” weather.

Although the slow, sub-hertz fluctuations in the Canberra “clear” weather data (Fig. 5) are much larger than seen in the Antarctic “ice haze” data, the power spectra show that the noise in the 1–2 Hz region is in fact larger in the “ice haze” spectrum, even though the total brightness is nowhere near as large as that seen from the Canberra clear sky. This reflects the low altitude and particulate nature of the ice haze, compared with the higher and slower fluctuations in atmospheric temperature and water vapor content that are responsible for the variations in the Canberra clear sky data.

The main effect of the “ice haze” that we can determine from these observations is to significantly increase the noise in the 1–2 Hz region of the power spectrum. By employing standard chopping techniques at a few hertz it should be possible to effectively remove this source of noise, leaving an elevated background compared with clear polar skies, but still well below that found at mid-latitude observing sites.

## 4. CONCLUSIONS

A successful mid-infrared site testing program was conducted at the US Amundsen-Scott South Pole Station, in 1996 January. From these observations it is clear that the high Antarctic Plateau is indeed a superb site for infrared astronomy. The sensitivity improvements achievable from the South Pole

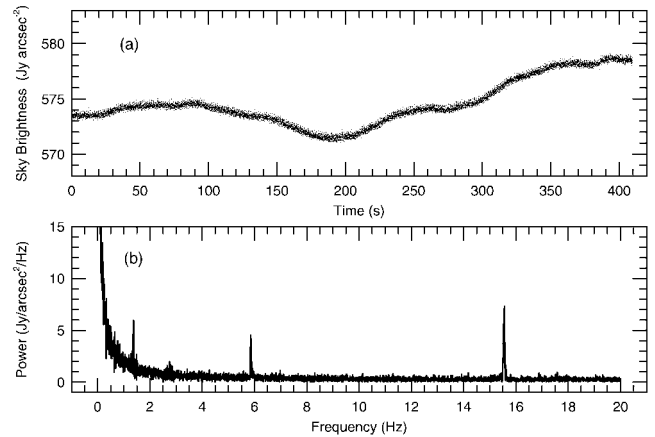


FIG. 7.—(a) Sky stability in the  $N$ -band at the South Pole during a period when “ice haze” was present. Again with 50 ms integrations, at  $0^\circ$  zenith distance. The sky is no longer as stable as in Fig. 4 (clear weather), but still much better than the sky stability at Canberra (Fig. 5). (b) Power spectrum vs. frequency from (a). The DC component has been removed from the power spectrum.

are much larger than would be predicted from the temperature difference, compared with a mid-latitude site alone. In the best parts of the  $8\text{--}13\ \mu\text{m}$  window the sky emissivity decreases by between a factor of 5–10 to around 0.5%–1% of the ambient  $-30^\circ\text{C}$  temperature. This is largely attributed to the reduction in the water vapor and aerosol content of the atmosphere. Combined with the simple temperature decrease factor of about 0.4 between a  $10^\circ\text{C}$  and  $-30^\circ\text{C}$  blackbody, this gives a total reduction in sky emission of 10–20. These improvements were obtained during the South Pole summer, so during the winter when temperatures drop to around  $-70^\circ$  and the water vapor content drops even lower, to around  $200\ \mu\text{m}$ , we might expect the sky brightness and emissivity to be even lower too, perhaps as low as 0.1% of a 200 K blackbody or  $780\ \text{mJy arcsec}^{-2}$ .

Under these conditions, the emissivity of the telescope is clearly going to dominate the sky emission by more than an order of magnitude, presenting new challenges to telescope and instrument construction to get total instrument emissivities to 1% or less. Currently, the lowest emissivity telescopes are of the order of 2%–3% (e.g., Gemini design specification). The extremely stable sky on the Antarctic Plateau means that chopping is probably unnecessary during clear weather and that for the first time mid-infrared astronomical observations could be usefully obtained in a stare mode. Removal of the need for an oscillating secondary would greatly simplify the construction of a large telescope, and make the goal of a 1% emissive telescope feasible. Nontraditional telescope designs (e.g., off-axis) and low-emissivity, multilayer coatings will also need to be considered in the attempt to keep the telescope emissivity low. Whatever the eventual achieved emissivity, a telescope on the cold Antarctic Plateau will always have the added benefit of being ambiently cooled to around  $-70^\circ$  during winter, sig-

nificantly reducing the telescope contribution to background compared with warmer sites.

Assuming the worst case Antarctic emissivity (i.e., summertime clear weather emissivity of 0.7% emissive sky, 2.5% emissive telescope, but an ambient temperature  $-70^{\circ}\text{C}$ ) an instrument at a telescope on the Antarctic Plateau would see a total background at  $11.5\ \mu\text{m}$  of around  $41\ \text{Jy arcsec}^{-2}$  (not including the emissivity of the instrument). For the best mid-latitude sites such as Mauna Kea (2.5% emissive sky, 2.5% emissive telescope, ambient temperature  $0^{\circ}\text{C}$ ) the background is around  $316\ \text{Jy arcsec}^{-2}$ . So a 2 m telescope on the Antarctic Plateau should have the sensitivity to extended sources of a Mauna Kea telescope with diameter about 15.5 m. It should be noted that there is a linear correspondence between sensitivity and telescope diameter (rather than area or aperture) for extended objects in the background-limited case. On point sources the “warm,” larger telescopes recover ground owing to their smaller diffraction limit, and in this case sensitivity scales as the telescope area, provided pixel scales are optimized to the diffraction limit size or smaller. So for point sources an Antarctic 2 m telescope only provides for the equivalent sensitivity of a 5.5 m mid-latitude telescope (under the same conditions as before). It should be noted that this comparison has been made on the basis of Mauna Kea emissivity measurements that were aimed primarily at measuring the emissivity of the telescope rather than the sky, although the sky emissivity is a critical component of the calculation. A definitive comparison must await properly controlled measurements made on Mauna Kea, which we hope to conduct in the future.

A further, significant, advantage for polar mid-infrared astronomy would be routine access to the  $20\ \mu\text{m}$  window, which is normally dominated by water vapor absorption and is only occasionally accessible from mid-latitude infrared observing sites, even for the best sites like Mauna Kea in Hawaii.

From the CVF spectra of Figure 2 it is clear that there is an optimal spectral region from about  $10.2$  to  $11.8\ \mu\text{m}$ , where the sky is darkest and sensitivity will be greatest. Under the Antarctic observing conditions, using a broadband filter such as the *N*-band filter is counterproductive, since it includes too much of the high-emissivity portion of the spectrum. Comparing observations of a source with a flat spectral distribution, the broadband filter gains by a factor  $(5/1.6)^{1/2}$  by virtue of its extra wavelength coverage. However, the average *N*-band emissivity is around 20% compared with less than 1% in the

optimal  $10.2$ – $11.8\ \mu\text{m}$  band, so overall the narrower but optimized band would provide a tenfold or more sensitivity improvement over the *N* band. It is worth noting that the S IV fine-structure line falls neatly into the optimized band, though unfortunately the Ne II line falls in a rather emissive part of the window, even at the South Pole.

Further site testing of the South Pole and the high Domes Circe and Argus is currently being conducted by the JACARA site testing program (Burton et al. 1996), with the deployment of an Automated Astronomical Site Testing Observatory (AASTO) to the South Pole in 1997 (Storey, Ashley, & Burton 1996<sup>1</sup>) and to Dome Circe in 1999. These site testing observations will undoubtedly encounter even lower sky brightness results and locate the best infrared observing site in the world. The next step is to build a telescope there that can take advantage of these conditions and provide the most sensitive mid-infrared observations achievable from the ground.

There are many acknowledgments to be made to those who contributed to the success of this site testing program at the South Pole. First, C. H. S. should thank Al Harper and Bob Lowenstein of CARA for agreeing to support this project and providing for all of the logistical support. Thanks also to Joe Rottman (CARA) and all the Antarctic Support Associates staff who assisted with the operation at the South Pole. Tony Peebles from the Electronics Laboratory in the School of Physics worked hard through the Christmas period to get the temperature monitor and control electronics ready in time for shipping to the Pole, and for this we am most grateful. The excellent reliability and operability of the instrument owes much to his talents. Thanks also to Jamie Lloyd (CARA) and Michael Burton (JACARA/UNSW) for their assistance and companionship at the South Pole. The MIRAS/NIMPOL instrumentation program was funded by a grant from the Australian Research Council (ARC), and C. H. S. was funded throughout this work by an ARC Research Fellowship.

This research was supported in part by the National Science Foundation under a cooperative agreement with the Center for Astrophysical Research in Antarctica (CARA), grant NSF OPP 89-20223. CARA is a National Science Foundation Science and Technology Center.

<sup>1</sup> Also <http://www.phys.unsw.edu.au/mcba/aasto.html>.

## REFERENCES

- Aitken, D. K., & Roche, P. F. 1982, MNRAS, 200, 217  
 Ashley, M. C. B., Burton, M. G., Storey, J. W. V., Lloyd, J. A., Bally, J., Briggs, J., & Harper, D. A. 1996, PASP, 108, 721  
 Burton, M. G., et al. 1996, Publ. Astron. Soc. Australia, 13, 33  
 Käufel, H. U., Bouchet, P., Van Dijsseldonk, A., & Weilenmann, U. 1991, Exp. Astron., 2, 115  
 Nguyen, H. T., Rauscher, B. J., Severson, S. A., Hereld, M., Harper, D. A., Lowenstein, R. F., Morozek, F., & Pernic, R. J. 1996, PASP, 108, 718  
 Smith, C. H., Aitken, D. K., & Moore, T. J. T. 1994, Proc. SPIE, 2198, 736  
 Smith, C. H., Moore, T. J. T., Aitken, D. K., & Fujiyoshi, T. 1996, Publ. Astron. Soc. Australia, 14, 179  
 Storey, J. W. V., Ashley, M. C. B., & Burton, M. G. 1996, Publ. Astron. Soc. Australia, 13, 35